Coupled global wind and tide driven coastal water levels and currents in Puerto Rico and the U.S. Virgin Islands

Juan Gonzalez-Lopez and J.J. Westerink
Department of Civil & Environmental Engineering & Earth Sciences
University of Notre Dame
Notre Dame, IN
Email: jgonza18@nd.edu

M. Canals and J.M. Morell
UPRM Center for Applied Ocean Science and Engineering
Department of Engineering Science and Materials & Department of Marine Sciences
University of Puerto Rico at Mayaguez

***Abstract*—A high-resolution, unstructured finite element hydrodynamic model was implemented with a focus on the regional dynamics of Puerto Rico and the U.S. Virgin Islands. Spatial resolution of the unstructured mesh is at least 100 m along all the coastlines of Puerto Rico and the U.S. Virgin Islands and reaches a resolution finer than 50 m in selected areas with complex coastlines. The model is forced with a global tide solution (TPXO8) and global atmospheric forcing provided by the NCEP Climate Forecast System (CFSv2) model. Inclusion of the global atmospheric forcing resulted in an increase of the model accuracy in modeling water levels. Atmospheric forcing was a necessary condition for the generation of currents and high frequency water level oscillations such as seiches. This newly developed hydrodynamic model for Puerto Rico and the U.S. Virgin Islands has applications for maritime users as the inclusion of global winds results in more accurate water levels as well as coastal currents, which were not able to be generated previously without the inclusion of atmospheric forcing. In addition, the generation of high frequency oscillations that have been observed in measurements allows for further study of local scale dynamics that have not been able to be previously replicated by numerical models in this region.**

I. Introduction

Although the circulation and transport into and out of the Caribbean Sea has been previously studied [1], [2], there is a lack in the study of the tidal regime, water levels, and coastal circulation of the region. To this date Kjerfve [3] has done the most comprehensive analysis of the tidal regime in the Caribbean Sea, and more recently Torres and Tsimplis have studied the long-term modulation of tides, seasonal sea level cycles, and sea level extremes in the Caribbean Sea [4]–[6]. In the past years there has been a significant increase in instrumentation and data availability in Puerto Rico and the Virgin Islands. Along with the computational capabilities to run high resolution models that can represent the complex coastlines of the region, this data availability allows for an in depth study that combines both numerical modeling and observations.

In this paper we present a summary of the results of a new high resolution, two-dimensional circulation model of Puerto Rico, Virgin Islands and the Caribbean. The focus is on the interaction between tidal and atmospheric forcing and its effect on water levels and currents. Water level and current observations through the region are used to give an overview of the range of processes that occur and then are used for comparison with the model to assess its skill. The generation of high frequency water level oscillations at locations where they are observed is explored, as is the necessity of using atmospheric forcing to generate this process as well as currents. The implications of these findings both in terms of the necessary forcing mechanisms in the numerical model and for the understanding of the observed coastal dynamics are discussed.

II. Hydrodynamic Model and Data Sources

A. Hydrodynamic Model

Modeling of water levels and currents was done using the ADCIRC finite element model. The model solves the two-dimensional, depth-integrated nonlinear shallow water equations. ADCIRC has been extensively validated for tidal constituent and storm surge water levels in the Gulf of Mexico, Florida, and the Atlantic Ocean, in addition to being used operationally as part of the ESTOFS forecast system [7]–[10]. The use of an unstructured mesh gives the advantage of solving for various physical scales on a single mesh. In our application these scales ranged from basin to shelf down to coastal and nearshore. The model was run in implicit mode with a timestep of 1 s, lateral eddy viscosity was set to 5 ms^{-2} and bottom friction was formulated as a quadratic bottom stress dependent on the bottom type at every mesh node.

A high resolution mesh was built using as a basis the EC2001 grid [7]. The open ocean boundary was extended further east to allow enough space between the boundary and the Lesser Antilles, which falls within our area of interest as transport between the Atlantic Ocean and the Caribbean Sea occurs through them. Because of their importance in the regional transport, the Lesser Antilles were resolved to a resolution of up to 250 m. Spatial resolution is finest at 30 m in

978-0-933957-43-5 ©2015 MTS

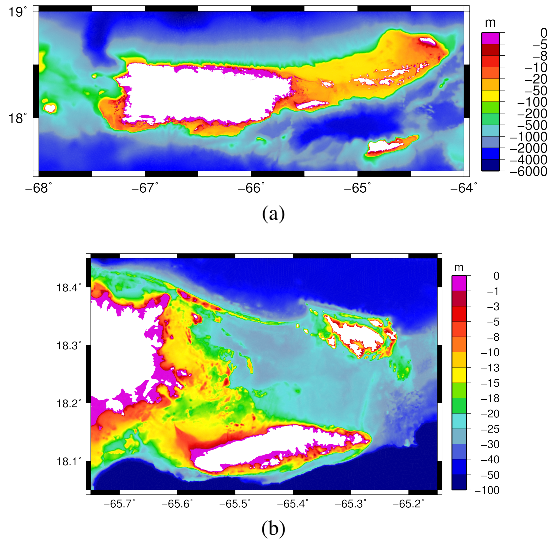

Fig. 1. Mesh bathymetry over (a) Puerto Rico and Virgin Islands and (b) detail of the bathymetry over the eastern coast of Puerto Rico.

some areas of Puerto Rico, with a resolution of at least 100 m along all the coastlines of Puerto Rico and the Virgin Islands. Figure 1 shows the mesh bathymetry over Puerto Rico and the Virgin Islands and the level of detail that has been achieved in representing the steep shelves, irregular coastlines, and shallow reef systems. To take into account the frictional effects of reefs and mangroves global maps of reef and mangrove coverages were included as attributes of the mesh [11], [12]. For reefs, a Manning's n value of 0.220 was used [13] and for mangroves the Manning's n was 0.400 [14].

B. Boundary Conditions and Atmospheric Forcing

The open ocean boundary was forced with tidal amplitudes and phases for each of the eight (M_2, K_2, N_2, S_2, O_1, K_1, S_1, P_1) principal tidal constituents. Amplitudes and phases were extracted from the OSU TPXO8-ATLAS [15] global tidal solution. The forcing constituents were referenced to the simulation time of January-November 2012 by computing the nodal factors and equilibrium arguments [16], [17].

Global atmospheric pressure and wind fields were obtained from NCEP's CFSv2 Climate Forecast System [18]. The fields covered the entirety of the mesh with a spatial resolution of 20 km and a temporal resolution of one hour. Both fields were ramped for a duration of 15 days using a hyperbolic tangent function where wind speeds and pressure increased from zero m/s and 1013 mb, respectively. This ramping was used to avoid generating any spurious oscillations. Atmospheric forcing was applied for the duration of the simulation.

C. Water Level and Currents Observations

To determine the skill of the model the water levels and currents were compared to observations. The broad distribution of instrumentation (Figure 2) in the Puerto Rico and U.S. Virgin Islands regions allows for data that represents conditions in the Atlantic Ocean and Caribbean Sea as well as through the transitions between them.

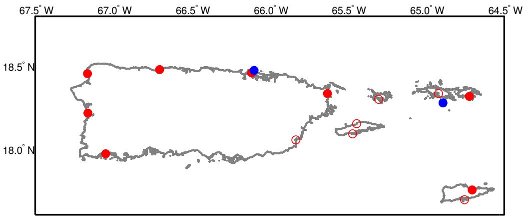

Fig. 2. Location of water level (red) and currents (blue) validation stations. Filled circles represent the locations that are shown in this paper.

Observed water levels were obtained from the NOAA National Ocean Service (NOS) tide gauges in Puerto Rico and the U.S. Virgin Islands. Water levels are measured every six minutes, which was the same interval used for model output. As we were interested in determining the effect of the inclusion of atmospheric forcing in the generation of high frequency oscillations, the power spectrum density was computed for both observed and modeled water levels. For this the Thomson multitaper method [19] was used on the monthly water level time series.

Currents were measured by the moored buoys operated by the Caribbean Coastal Ocean Observing System (CariCOOS). Buoys are equipped with ADCPs that sample at every meter through the water column. Depths at the buoys are 32 m in buoy PR206 (north of San Juan) and 44 m in buoy VI105 (south of St. John). Current speed and direction were depth-averaged to be used for comparison with ADCIRC.

III. Results

A. Water Levels

Water levels showed varied responses to the atmospheric forcing. These responses depended on the particular location of each validation station as well as the agreement of the CFSv2 global atmospheric fields with the observed meteorological conditions. Figure 3 shows the modeled and observed water levels for three different time snapshots at Christianted Harbor (St. Croix), Magueyes Island (Puerto Rico) and Lameshur Bay (St. John). In general the inclusion of atmospheric forcing forcing resulted in better accuracy of the modeled water levels, but this increase in accuracy was not limited only to the direct comparison of the water levels, but also to the generation of other physical phenomena that otherwise are not generated with purely tidal forcing.

In Christiansted Harbor the modeled water levels with the tidal and atmospheric forcing better followed the behavior of the observed water levels. This is more evident during January 16-21 and 28-31, where the modeled water levels had lower values relative to the tide-only forcing water levels, similar to what was observed. This gives an indication of how the atmospheric fields can have a modulating effect on the water levels in a non tropical cyclone situation.

Figure 3(b) shows how the atmospheric forcing greatly increased the accuracy of the model at Magueyes Island during October 10-15, 2012. Additionally, the high frequency

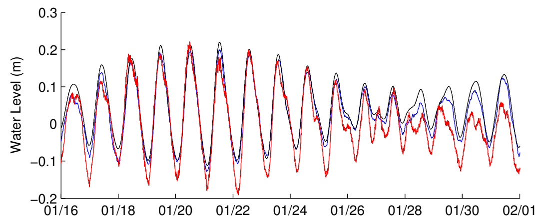

(a)

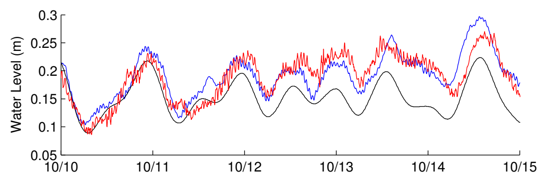

(b)

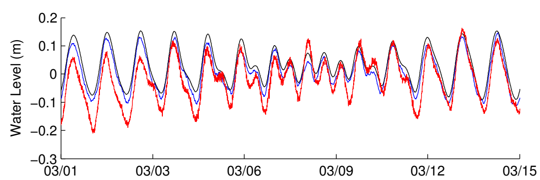

(c)

Fig. 3. Observed and modeled water levels in (a) Christiansted Harbor, (b) Magueyes Island, and (c) Lameshur Bay. Black lines represent ADCIRC with only tide forcing, blue lines represent ADCIRC with tide and atmospheric forcing, and red line represents the observed water levels.

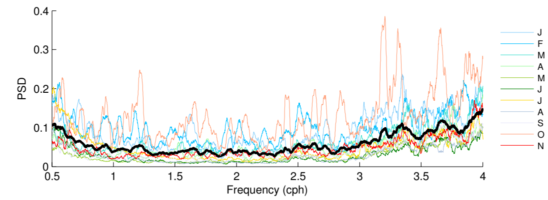

(a)

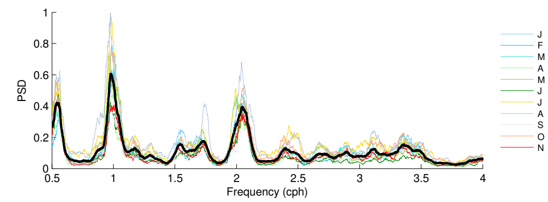

(b)

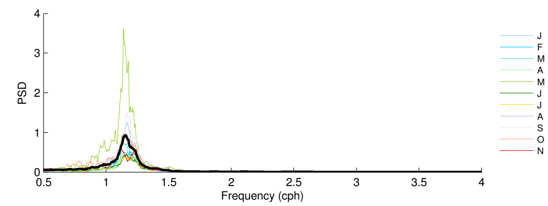

(c)

Fig. 4. Observed high frequency spectrum of water levels in (a) Arecibo, (b) Fajardo, and (c) Magueyes Island. Colored lines represent January-November 2012 and black line represents the mean power spectrum density.

oscillations that are evident in the observed water levels were also present in the model results. This location is a good example of how different the ADCIRC solution can be by just including atmospheric forcing. This difference is seen in the actual water levels plus the non-linear interactions of winds and pressure with the tides and the shelf.

The results in Lameshur Bay are similar to those in Christiansted Harbor. Figure 3(c) shows that through March 1-15 the modeled water levels with atmospheric forcing had a better accuracy and followed the behavior of the observations. A difference on this station is that the observed water levels shows strong high frequency oscillations only at some times, contrary to Magueyes Island where the oscillations are predominant through the record. This variability in high frequency oscillations will be explored next.

B. High Frequency Water Level Oscillations

The inclusion of atmospheric forcing in ADCIRC resulted in the generation of high frequency oscillations (ranging between 0.5 and 2.0 cph) which were not generated when the model was forced purely with tidal forcing. As high frequency oscillations were also present in the observations at some locations we decided to further investigate these oscillations and how they compared between model and observations.

Figure 4 shows the observed power spectrum at three locations in Puerto Rico: Arecibo, Fajardo, and Magueyes Island during January-November 2012. These three locations serve as an example of the different characteristics of the high frequency oscillations that are observed through the region. The Arecibo spectrum shows a strong monthly variability, with no predominant peaks in the record. This station is located in the Atlantic coast of Puerto Rico and is exposed to the wave activity that hit this coast, which can explain the monthly variability in the spectrum.

In Fajardo the spectrum shows a combination of predominant peaks through the range of 0.5 - 4.0 cph with some monthly variability. The monthly variability includes both higher amplitudes in the predominant peaks as well as energy at frequencies that are not the predominant peaks. This station is located in the Northeast coast of Puerto Rico, influenced both by the Atlantic Ocean and the transition into the Caribbean Sea through the Virgin Islands shelf, and protected by a long reef chain that faces the Atlantic Ocean. The combination of limited exposure to the Atlantic wave fields (due to the reef protection) while at the same time being on the shelf can explain the predominant energy peaks with some variability caused by the wave fields that are not completely dissipated by the reef.

Magueyes Island is located in the southwestern coast of Puerto Rico, in a relatively broad shelf of a width of 12 km and mean depth of 18 m. The spectrum in Magueyes Island had a predominant single peak at around 1.20 cph (50 min period), which coincides with the fundamental resonant period

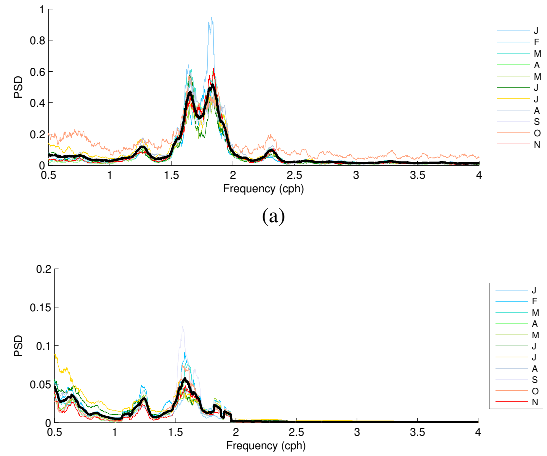

(a)

(b)

Fig. 5. High frequency spectrum of water levels in Mayaguez: (a) observed and (b) ADCIRC. Colored lines represent January-November 2012 and black line represents the mean power spectrum density.

of Magueyes Island [20]. There was little energy at any other frequencies and with little monthly variability. This location is surrounded by reefs and cays that protect the coast from wave action, resulting in a unimodal spectrum with a peak in the shelf fundamental period. The only notable exception was during May 2012, where the amplitude of the spectrum was much higher than during any other month.

The high frequency spectrum of the ADCIRC water levels with atmospheric forcing are shown in Figures 5 and 6. In Mayaguez (Figure 5) the shape of the ADCIRC spectrum resembles the observed spectrum, with a peak at 1.24 cph (55 min period) and another peak at 1.58 cph (38 min period). The main difference between the observed and the modeled spectrum is that ADCIRC does not completely generates the second peak near the 2 cph frequency, although there is a small amount of energy being generated at this frequency.

In the case of Magueyes Island (Figure 6) the ADCIRC spectrum fully resembles the observed unimodal spectrum centered about 1.20 cph. As this is the same as the natural resonant period of Magueyes Island, this indicates that resonant motions can not be forced only by tides, as the tide-only ADCIRC spectrum did not showed any energy at this frequency. This means that the atmospheric forces are at least in part a contributor to the generation of the resonant motions in Magueyes Island.

C. Currents

The most notable result of including the atmospheric forcing in ADCIRC was the generation of currents, which with tide-only forcing had very low speeds. The current speed response to the atmospheric forcing at the two studied locations also gives light as to the driving mechanisms of the currents at each location and the variability that is observed in the region. In both cases the accuracy of the current speeds increased with the atmospheric forcing, but the influence of the atmospheric forcing in San Juan was greater than in St John.

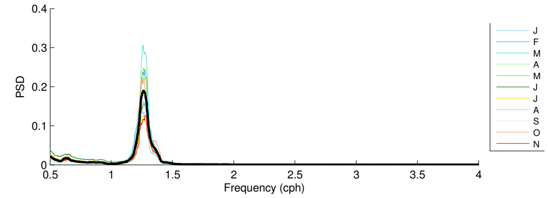

Fig. 6. ADCIRC high frequency spectrum of water levels in Magueyes Island. Compare to the observed spectrum in Figure 4(c). Note the difference in scale.

Figure 7 shows the observed and modeled currents during July 2012. In San Juan it is evident how the atmospheric forcing caused an increase in the current speeds. With tide-only forcing the current speeds were almost zero, while with atmospheric forcing the speeds increased and accurately followed the behavior of the observed currents. The model did not captured all the daily peaks, but this can be due to the resolution limits of the global atmospheric model as well as the local winds that change rapidly through the day. The dramatic difference between the ADCIRC speeds makes it clear that in San Juan the tidal influence in the current speeds is very small, being dominated by the atmospheric forcing.

Currents in St. John also increased in accuracy with the atmospheric forcing, although the contribution of the tidal forcing to the currents was higher than in San Juan. The tide-only ADCIRC currents were proportionally higher than those in San Juan, having speeds closer to the observed currents than they were in San Juan. With atmospheric forcing the currents had a better accuracy, with an increase in magnitude and following the patterns of the observations. As the St. John buoy is located in the Virgin Islands shelf, contrary to San Juan which is exposed to the Atlantic deep waters, the tidal currents are stronger. The good agreement of the model with the overall behavior of the observations in St. John leads to think that the consistently lower speeds in the model could be caused by the global model winds not capturing the local effects near the buoy.

IV. Discussion

The results show that the use of atmospheric forcing along with the tidal forcing in ADCIRC increases the accuracy of the model. This increase in accuracy is seen in both the modeled water levels and currents, and the effect of the atmospheric forcing is further seen in the generation of other observable phenomena such as high frequency oscillations in the water levels. Without atmospheric forcing neither strong enough currents nor high frequency oscillations were generated. In addition, the atmospheric forcing was able to generate observed localized phenomena that characterizes different locations in the Atlantic Ocean, the Caribbean Sea and the transition between them.

Water levels from ADCIRC were able to accurately model the observed water levels as well as the local characteristics of the three locations shown in Figure 3. When atmospheric forcing was applied all three locations had better agreement

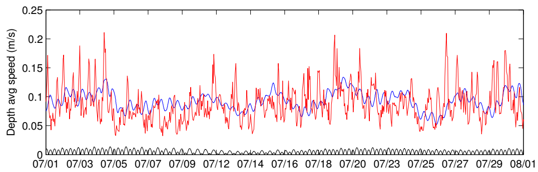

(a)

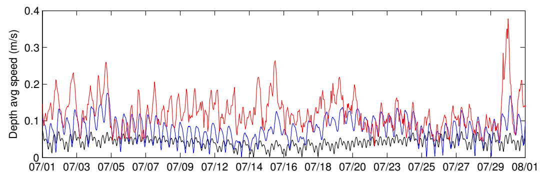

(b)

Fig. 7. Observed and modeled current speeds in (a) San Juan and (b) St. John during July 2012. Black lines represent ADCIRC with only tide forcing, blue lines represent ADCIRC with tide and atmospheric forcing, and red line represents the observed currents.

with the observed data than when forcing ADCIRC with tides only. The level of detailed representation of the bathymetry in our high resolution mesh is illustrated by how the model did a good job in capturing the characteristics of each location, i.e. generating oscillations in the natural resonant period at Magueyes Island where they are observed, while not generating similar oscillations where they do not occur. This shows that a fine spatial representation and large-scale atmospheric forcing can recreate a broad range of physical phenomena at temporal scales that range from days to minutes in the Puerto Rico and Virgin Islands region.

Currents and high frequency oscillations were only generated when atmospheric forcing was used. As the tidal range in Puerto Rico and the U.S. Virgin Islands is small (in the order of 0.3 m), this would indicate that the main driver of these two processes are the winds and atmospheric pressures. The case of the currents in San Juan is particularly of interest as this buoy is located at the edge of the very narrow shelf North of Puerto Rico (about 3 km wide), where it is exposed to the circulation from the deep waters that follow right after the shelf. Tide-only forcing barely generated any currents at this location, while tide and atmospheric forcing resulted in very good agreement with the observations, meaning that at least during July 2012, circulation in this buoy was in great part driven by local and regional winds and that a two-dimensional circulation model provides a good agreement.

V. Conclusion

A high resolution, two-dimensional circulation model of Puerto Rico, Virgin Islands, and the Caribbean has been developed. This model accurately captures the water level and circulation processes of the region. When coupled to a global atmospheric model, the model is able to generate the observed high frequency oscillations that are observed at the tide gauges. Atmospheric coupling was proven to be necessary for the generation of currents, and the modeled currents agreed well with the observations in San Juan and St. John. Seiching at Magueyes Island was also captured by the model, as well as a good representation of the spectrum at high frequencies in Mayaguez. It was our intent to show in detail a series of locations that are representative of the range and characteristics of processes that occur in the region and a full validation of the different components of the model will be treated in subsequent papers.

Acknowledgments

The authors would like to thank the Southeastern Universities Research Association (SURA), NOAAs National Ocean Service and the U.S. IOOS Coastal and Ocean Modeling Testbed for supporting the work presented here. High performance computing resources were provided by the Computing Research Center (CRC) at University of Notre Dame, the Texas Advanced Computing Center (TACC) at The University of Texas at Austin and the Extreme Science and Engineering Discovery Environment (XSEDE) grant number TG-DMS080016N.

References

[1] W. Wilson and W. E. Johns, "Velocity structure and transport in the Windward Islands Passages," *Deep Sea Research Part I: Oceanographic Research Papers*, vol. 44, no. 3, pp. 487–520, Mar. 1997. [Online]. Available: http://www.sciencedirect.com/science/article/pii/S0967063796001136

[2] W. E. Johns, T. L. Townsend, D. M. Fratantoni, and W. Wilson, "On the Atlantic inflow to the Caribbean Sea," *Deep Sea Research Part I: Oceanographic Research Papers*, vol. 49, no. 2, pp. 211–243, feb 2002. [Online]. Available: http://dx.doi.org/10.1016/S0967-0637(01)00041-3

[3] B. Kjerfve, "Tides of the Caribbean Sea," *Journal of Geophysical Research*, vol. 86, 1981.

[4] R. R. Torres and M. N. Tsimplis, "Tides and long-term modulations in the Caribbean Sea," *J. Geophys. Res.*, vol. 116, no. C10, 2011. [Online]. Available: http://dx.doi.org/10.1029/2011JC006973

[5] ——, "Seasonal sea level cycle in the Caribbean Sea," *Journal of Geophysical Research*, vol. 117, no. C7, p. C07011, Jul. 2012. [Online]. Available: http://doi.wiley.com/10.1029/2012JC008159

[6] ——, "Sea level extremes in the Caribbean Sea," *Journal of Geophysical Research: Oceans*, vol. 119, no. 8, pp. 4714–4731, aug 2014. [Online]. Available: http://dx.doi.org/10.1002/2014JC009929

[7] A. Mukai, J. Westerink, R. Luettich, and D. Mark, "A Tidal Constituent Database for the Western North Atlantic Ocean, Gulf of Mexico and Caribbean Sea," U.S. Army Engineer Research and Development Center, Vicksburg MS, Report ERDC/CHL TR-02-24, 2002.

[8] Y. Funakoshi, S. C. Hagen, and P. Bacopoulos, "Coupling of Hydrodynamic and Wave Models: Case Study for Hurricane Floyd (1999) Hindcast," *Journal of Waterway, Port, Coastal, and Ocean Engineering*, vol. 134, no. 6, pp. 321–335, Nov. 2008. [Online]. Available: http://ascelibrary.org/doi/abs/10.1061/(ASCE)0733-950X(2008)134:6(321)

[9] J. C. Dietrich, J. J. Westerink, A. B. Kennedy, J. M. Smith, R. E. Jensen, M. Zijlema, L. H. Holthuijsen, C. Dawson, R. A. Luettich, M. D. Powell, V. J. Cardone, A. T. Cox, G. W. Stone, H. Pourtaheri, M. E. Hope, S. Tanaka, L. G. Westerink, H. J. Westerink, and Z. Cobell, "Hurricane Gustav (2008) Waves and Storm Surge: Hindcast, Synoptic Analysis, and Validation in Southern Louisiana," *Monthly Weather Review*, vol. 139, no. 8, pp. 2488–2522, Aug. 2011. [Online]. Available: http://journals.ametsoc.org/doi/abs/10.1175/2011MWR3611.1

[10] Y. Funakoshi, J. Feyen, F. Aikman, H. Tolman, A. van der Westhuysen, A. Chawla, I. Rivin, and A. Taylor, "Development of extratropical surge and tide operational forecast system estofs," in *Estuarine and Coastal Modeling*. American Society of Civil Engineers, nov 2012. [Online]. Available: http://dx.doi.org/10.1061/9780784412411.00012

[11] C. Giri, E. Ochieng, L. L. Tieszen, Z. Zhu, A. Singh, T. Loveland, J. Masek, and N. Duke, “Status and distribution of mangrove forests of the world using earth observation satellite data,” *Global Ecology and Biogeography*, vol. 20, no. 1, pp. 154–159, 2011. [Online]. Available: http://dx.doi.org/10.1111/j.1466-8238.2010.00584.x

[12] M. Kendall, M. Monaco, K. Buja, J. Christensen, C. Kruer, M. Finkbeiner, and R. Warner, “Methods Used to Map the Benthic Habitats of Puerto Rico and the U.S. Virgin Islands,” U.S. National Oceanic and Atmospheric Administration (NOAA). National Ocean Service (NOS), National Centers for Coastal Ocean Science (NOS) Biogeography Program, Silver Spring, MD., Benthic Habitats of Puerto Rico and the U.S. Virgin Islands., 2001.

[13] A. B. Kennedy, J. J. Westerink, J. M. Smith, M. E. Hope, M. Hartman, A. A. Taflanidis, S. Tanaka, H. Westerink, K. F. Cheung, T. Smith, M. Hamann, M. Minamide, A. Ota, and C. Dawson, “Tropical cyclone inundation potential on the Hawaiian Islands of Oahu and Kauai,” *Ocean Modelling*, vol. 52-53, pp. 54–68, aug 2012. [Online]. Available: http://dx.doi.org/10.1016/j.ocemod.2012.04.009

[14] E. Wolanski, Y. Mazda, and P. Ridd, *Mangrove Hydrodynamics*. American Geophysical Union, 2013, pp. 43–62. [Online]. Available: http://dx.doi.org/10.1029/CE041p0043

[15] G. D. Egbert, A. F. Bennett, and M. G. G. Foreman, “TOPEX/POSEIDON tides estimated using a global inverse model,” *J. Geophys. Res.*, vol. 99, no. C12, p. 24821, 1994. [Online]. Available: http://dx.doi.org/10.1029/94JC01894

[16] P. C. Kerr, A. S. Donahue, J. J. Westerink, R. A. Luettich, L. Y. Zheng, R. H. Weisberg, Y. Huang, H. V. Wang, Y. Teng, D. R. Forrest, A. Roland, A. T. Haase, A. W. Kramer, A. A. Taylor, J. R. Rhome, J. C. Feyen, R. P. Signell, J. L. Hanson, M. E. Hope, R. M. Estes, R. A. Dominguez, R. P. Dunbar, L. N. Semeraro, H. J. Westerink, A. B. Kennedy, J. M. Smith, M. D. Powell, V. J. Cardone, and A. T. Cox, “U.S. IOOS coastal and ocean modeling testbed: Inter-model evaluation of tides, waves, and hurricane surge in the Gulf of Mexico,” *Journal of Geophysical Research: Oceans*, vol. 118, no. 10, pp. 5129–5172, oct 2013. [Online]. Available: http://dx.doi.org/10.1002/jgrc.20376

[17] P. Schureman, “Manual of harmonic analysis and prediction of tides,” U.S. Dept. of Commer., Coast and Geodetic Surv., Washington, D. C., Special Publication No. 98, 1958.

[18] S. Saha, S. Moorthi, X. Wu, J. Wang, S. Nadiga, P. Tripp, D. Behringer, Y.-T. Hou, H. ya Chuang, M. Iredell, M. Ek, J. Meng, R. Yang, M. P. Mendez, H. van den Dool, Q. Zhang, W. Wang, M. Chen, and E. Becker, “The NCEP Climate Forecast System Version 2,” *Journal of Climate*, vol. 27, no. 6, pp. 2185–2208, mar 2014. [Online]. Available: http://dx.doi.org/10.1175/JCLI-D-12-00823.1

[19] D. Thomson, “Spectrum estimation and harmonic analysis,” *Proceedings of the IEEE*, vol. 70, no. 9, pp. 1055–1096, Sept 1982.

[20] G. S. Giese, D. C. Chapman, P. G. Black, and J. A. Fornshell, “Causation of Large-Amplitude Coastal Seiches on the Caribbean Coast of Puerto Rico,” *Journal of Physical Oceanography*, vol. 20, no. 9, pp. 1449–1458, Sep. 1990. [Online]. Available: http://journals.ametsoc.org/doi/abs/10.1175/1520-0485(1990)020%3C1449%3ACOLACS%3E2.0.CO%3B2